

## Deeper insight into phase relations in ultrathin Pb films

Ro-Ya Liu,<sup>1,2</sup> Angus Huang,<sup>3</sup> Chien-Chung Huang,<sup>3</sup> Chang-Yeh Lee,<sup>2</sup> Chung-Huang Lin,<sup>3</sup> Cheng-Maw Cheng,<sup>2</sup> Ku-Ding Tsuei,<sup>2</sup> Horng-Tay Jeng,<sup>3</sup> Iwao Matsuda,<sup>1</sup> and S.-J. Tang<sup>3,2,\*</sup>

<sup>1</sup>Institute for Solid State Physics, the University of Tokyo, Kashiwa, Chiba 277-8581, Japan

<sup>2</sup>National Synchrotron Radiation Research Center, Hsinchu 30076, Taiwan

<sup>3</sup>Department of Physics, National Tsing Hua University, Hsinchu 30013, Taiwan

(Received 4 March 2015; revised manuscript received 25 August 2015; published 11 September 2015)

Films of Pb(111) with thickness ranging from 1 to 16 monolayers (ML) were grown on Ge(111) and examined by angle-resolved photoemission spectroscopy. The measured thickness dependences of the work function and surface energy from the same set of samples were both well described by damped sinusoidal oscillatory functions with the same period, but the oscillation phases differ by 1/4 period between the two quantities, as judged by the node positions. This difference agrees with the prediction of a generic quantum-well model. The varied node positions of damped oscillations of the work function and surface energy were examined in terms of the details of Pb subband dispersions, indicating the different roles of the density of states at the Fermi level to both thin-film properties. The surface dipoles of Pb films were found to have no relevant effects on the phase shift of thickness-dependent work functions except for the amplitudes of oscillations. The total boundary phase shifts of the quantum well states, extracted from the energy positions of the quantum-well states for both Pb/Ge(111) and freestanding Pb films, are compared and related to the thickness-dependent work function and surface energy.

DOI: 10.1103/PhysRevB.92.115415

PACS number(s): 73.30.+y, 68.60.Dv, 73.21.Fg, 79.60.Dp

### I. INTRODUCTION

Metallic films are essential elements for nanodevices. When the films become very thin, their properties can be substantially altered by quantum size effects (QSE). Large variations as a function of film thickness have been reported in the work function [1], thermal stability [2], effective mass [3,4], electron-phonon coupling [5,6], superconducting transition temperature [7], and surface reactivity [8]. Boundary effects at the surface and the interface cause the electronic energy states along the surface normal to become discrete in momentum and energy, forming so-called quantum well states (QWS), which evolve with film thickness.

In preceding theoretical work, Schulte demonstrated theoretically thickness-dependent oscillations in work function of a jellium film with a period of 1/2 of the Fermi wavelength ( $\lambda_F/2$ ) [9]. When a QWS subband crosses the Fermi level and becomes occupied by electrons, a sudden change in the density of states (DOS) at the Fermi level  $E_F$  induces a local minimum in the work function. Based on fairly general arguments, one can infer that all physical properties of films should oscillate as a function of film thickness, but the oscillation amplitude damps out at large thicknesses toward the bulk limit. These general features were confirmed and elaborated in a number of theoretical and experimental studies; beating patterns due to noninteger periods of oscillations were demonstrated [10–18].

Nevertheless, interesting questions remain. At least four parameters are needed to describe a damped oscillatory function: amplitude, damping factor, period, and phase shift. These quantities can be inferred from a generic free electron-gas model [10,14,15], and the period of oscillation has been intensively studied [11]. However, the phases of oscillation related to different physical properties are still under debate. The standard quantum-well model [19] predicts a phase offset of 1/4 of a period between the surface energy and work

function, and this relationship appears to hold well in the case of Ag films on Fe(100) [2], but the relevant experimental data were relatively limited. Further testing is highly desirable. For Pb films grown on Ge or Si, oscillations have been observed over a very wide thickness range, and it would be a good case for testing the phase relation. A recent scanning tunneling microscopy (STM) study by Kim *et al.* of the local work functions (LWF) of Pb films concluded an anomalous phase relation between the work function and surface energy oscillations [20], which appeared to contradict the general phase rule. However, their results were different from another STM study of the same system by Qi *et al.* [21]. It is still unclear if the disagreement is due to technical issues of STM measurements [22], differences in sample preparation conditions, or limitations of the quantum-well model.

To resolve this issue, we have performed an angle-resolved photoemission spectroscopy (ARPES) study of the quantum well state energies [23], work function, and thermal stability of Pb films grown on Ge(111). Because our measurements of the different quantities are performed on the same set of samples, the results are not affected by sample differences. The film thickness used in our experiment ranges from 1 to 16 monolayers (ML) in small steps in order to resolve atomic layer increments. The results confirm the phase offset by 1/4 period between the work function and surface energy oscillations. The cause of this offset, a surface-dipole effect on the thickness-dependent work function, and a universal relation among the phase shifts of QWS energy, work function, and surface energy were investigated.

### II. METHODS

The photoemission measurements were performed using a Scienta R3000 ARPES analyzer with photons of energy 21.2 eV from a He lamp or synchrotron radiation from beam line 21B1-U9 at the National Synchrotron Radiation Research Center (NSRRC) in Taiwan. A highly doped *n*-type Ge(111)

\*Corresponding author: sjtang@phys.nthu.edu.tw

wafer with dopant concentration of  $10^{17}\sim 10^{18} \text{ cm}^{-3}$  was used as a substrate. It was cleaned *in situ* to yield a Ge(111)- $c(2\times 8)$  surface [23] and further processed by Pb deposition and annealing to yield a Pb/Ge(111)- $(\sqrt{3}\times\sqrt{3})R30^\circ$  reconstructed surface in the so-called  $\beta$  phase [24]. Further Pb deposition was performed with the substrate maintained at 123 K. The Pb film thickness quoted below includes the monolayer Pb of the  $\beta$  phase. Discrete evolution of the quantum well peaks for increasing Pb coverage as observed by ARPES in the normal-emission direction permits absolute determination of the film thickness.

First-principles calculations of the band structure, work function, and surface energy of freestanding Pb films were performed using the Vienna *Ab initio* Simulation Package (VASP) based on density functional theory with pseudopotentials and plane waves. Generalized gradient approximation (GGA) and local density approximation (LDA) [25,26] were used, respectively, to treat the electron exchange and correlation interaction. The cutoff energy was 144 eV, and the lattice constant used for Pb was 5.03 Å (4.87 Å) for GGA (LDA). Interlayer relaxation was allowed in both calculations.

### III. RESULTS AND DISCUSSION

#### A. Photoemission measurement

Figure 1(a) shows the onsets of the energy distribution curves (EDCs) for Pb films of 5 and 6 ML taken with a bias of  $-6$  V applied to the sample. The onset kinetic energies

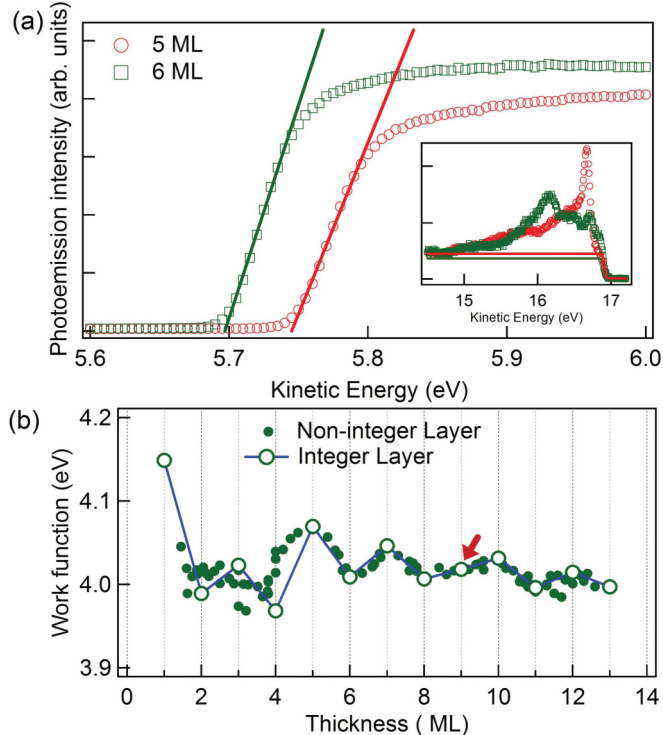


FIG. 1. (Color online) (a) Cutoff spectra showing the onset of EDCs for 5- and 6-ML Pb films on Ge(111). The inset shows the corresponding spectra near the Fermi edges. The solid fitted lines indicate the positions of onsets and the Fermi edges. (b) The measured work functions as a function of thickness ranging from 1 to 13 ML for Pb thin films on Ge(111).

are 5.75 and 5.70 eV for the 5- and 6-ML films, respectively. Thus, the difference in work function between the two cases is 0.05 eV. More generally, the work function  $W$  is given by

$$W = h\nu - [KE(E_F) - KE(\text{onset})], \quad (1)$$

where  $h\nu$  is the photon energy and  $KE(E_F)$  is the kinetic energy of the Fermi level [inset in Fig. 1(a)]. The extracted work function for Pb films as a function of thickness is shown in Fig. 1(b). Sharp changes in work function are seen at discrete atomic layer thicknesses, a behavior consistent with layer-by-layer growth. Evidently, the work function exhibits quasibilayer oscillations, in qualitative agreement with previous studies. Below 9 ML, the work function is a minimum at even layers and a maximum at odd layers. The trend reverses above 9 ML. The crossover at 9 ML (indicated by a red arrow) is one of the node positions of the beating pattern that has been discussed thoroughly in prior studies [10–18]. The thick-film or bulk limit of the work function is about 4.0 eV.

Figures 2(a) and 2(b) show a series of temperature-dependent EDCs for 5- and 7-ML Pb films on Ge(111) as the sample was annealed from 123 to 283 K. The QWS near the Fermi level in each case exhibits a split line shape due to interaction with the Ge band edges [23]. As observed, the evolution of the QWS with annealing temperature behaves differently for the two cases. The QWS for the 5-ML film decreases slightly in intensity until 253 K, beyond which the intensity drops abruptly. At 273 K, a new QWS peak corresponding to 10 ML emerges at  $-0.45$  eV. For the 7-ML film, the intensity of the QWS peak drops abruptly at 223 K, and a new QWS peak corresponding to 8 ML emerges at  $-0.61$  eV. In the latter case, the intensities of the QWS peaks for 7 and 8 ML as a function of annealing temperature are displayed in Fig. 2(c). A break is seen at 217 K for both curves, which is identified as the maximum stability temperature beyond which the 7 ML film decomposes into other thicknesses including 8 ML. Figure 2(d) presents measured thermal-stability (stability temperature) data of Pb films ranging from 3 to 16 ML. Two even-odd crossover positions at 5 and 14 ML are indicated by arrows. The appearance of 10-ML QWS at elevated annealing temperature in Fig. 2(a) indicates the relatively high stability of this thickness, as revealed in Fig. 2(d). The broad peak at  $-1.32$  eV in the same figure that emerges above about room temperature is associated with Pb/Ge(111)- $\sqrt{3}\times\sqrt{3}R30^\circ$ , which also emerges due to the decomposition of the Pb film [4,23]. The node position at 14 ML agrees with the finding of a previous STM study [17].

A comparison of Figs. 1(b) and 2(d) reveals that the crossover or node position for the work function sits just about midway between two neighboring node positions for the thermal stability. This is consistent with a phase shift offset of  $1/4$  period of oscillation between the two cases. Table I summarizes the measured and calculated node positions for Pb films on different substrates reported previously. Our measured results are very close to those reported in a previous first-principles calculation [11]. For most of the systems listed, the relative difference between node positions of work function and surface energy are about 4 or 5 ML with the exception from the STM results on Pb/Si(111) reported in [20].

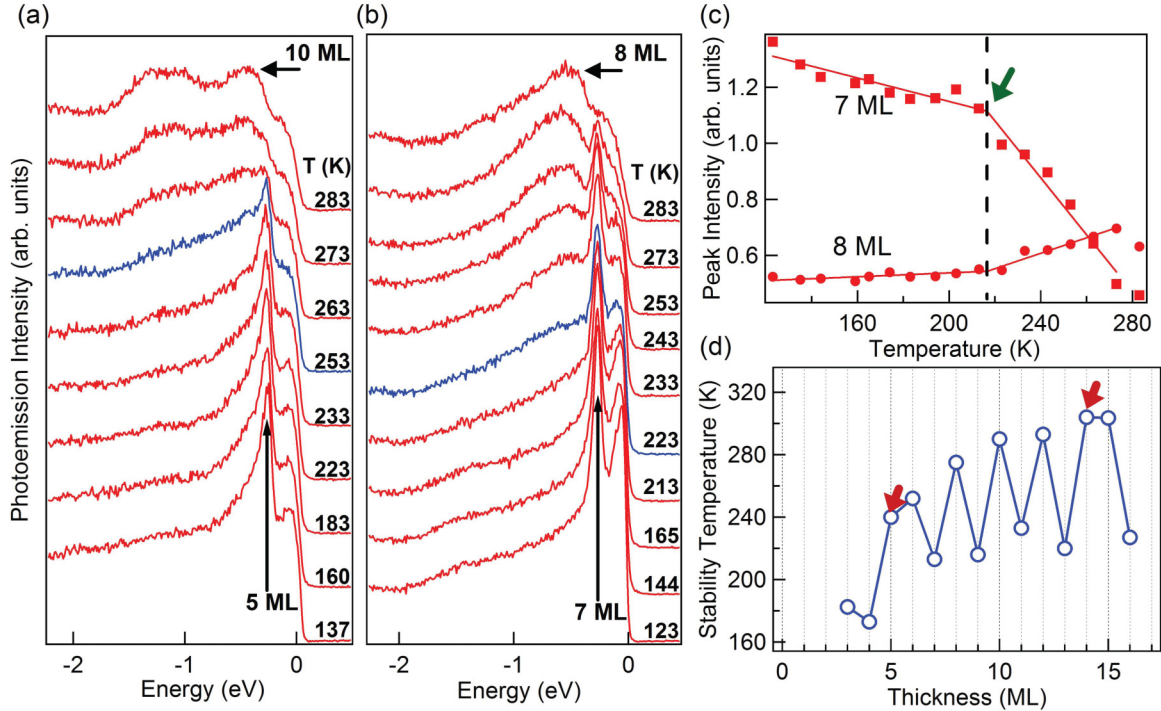


FIG. 2. (Color online) Evolution of EDCs with elevated temperatures from 123 to 283 K for (a) 5-ML and (b) 7-ML Pb films on Ge(111). The blue EDCs indicate the films near threshold temperature for collapsing. (c) Peak intensities of QWS for 7 and 8 ML as a function of temperature. The arrow and dashed line indicate the threshold temperature for the collapse of 7 ML and growth of 8 ML. The solid lines indicate line fitting. (d) The thermal stability indicated by threshold temperatures as a function of thickness ranging from 3 to 16 ML.

## B. Discussion

The experimental work function and thermal stability versus integer thickness  $N$  can each be fitted by the following damped sinusoidal functions [19] for the quasibilayer oscillations [Eq. (2)] and envelope functions or beating patterns [Eq. (3)]

$$F1(N) = \frac{A \sin(2k_F N d + \phi) + B}{N^\alpha} + C, \quad (2)$$

$$F2(N) = \frac{\pm A \sin(2k_E N d - \phi) + B}{N^\alpha} + C, \quad (3)$$

The layer spacing of Pb (111) film, or the ML thickness,  $d = 2.86 \text{ \AA}$ . The value used for Fermi wave vector  $k_F$  of Pb in Eq. (2) is  $0.486 \text{ \AA}^{-1}$ , which is defined with respect to the zone boundary at the  $L$  symmetry point. Another wave vector  $k_E$  in Eq. (3) for the envelope function is defined to be  $\frac{\pi}{2d} - k_F$ . The corresponding wavelengths (or period) for  $F1(N)$  and

$F2(N)$  are 2.26 ML and 17.4 ML. The decay power  $\alpha$  [9,10] can be taken to be around 1 for the work function and 2 for the surface energy over the thickness range of interest. Here,  $\phi$  is a phase shift, which can be different for the work function and thermal stability.

The fits and the data for the work function and stability temperature are shown in Figs. 3(b) and 3(c), respectively. At low coverages (1–3 ML), large deviations between the fits and data are evident, which can be attributed to the breakdown of the simple model at such small thicknesses. We will ignore this range in our analysis. It also needs to be noted that the fitted node positions are deviated from those determined by crossover positions by no more than 1 ML. The phase shifts for the work function and the thermal stability  $\phi_w$  and  $\phi_{TS}$  obtained from the fitting are 0.43 and  $-1.18$ , respectively. The difference is  $1.61$ , or  $0.51\pi$ , which matches well the  $1/4$  of a period as predicted by the quantum-well model. For the quasibilayer oscillation with the period of 2.26 ML,

TABLE I. Collection of the node positions (ML) for thickness-dependent surface energies and work functions in previous work on Pb films.

	Freestanding <sup>a</sup>	Freestanding <sup>b</sup>	Freestanding <sup>c</sup>	Pb/Cu(111) <sup>a</sup>	Pb/Ge(111) <sup>a</sup>	Pb/Ge(111) <sup>d</sup>	Pb/Si(111) <sup>e</sup>
E <sub>S</sub>	8/17	8/17	4/11	5/12	5/13/23	5/14	14/23
W	4/13	3/12/22	8/15	9/16	9/18	9	12/20
E <sub>S</sub> –W	4/-5/4	5/-4/5/-5	-4/3/-4	-4/3/-4	-4/4/-5/5	-4/5	2/-6/3

<sup>a</sup>Ref. [11].

<sup>b</sup>Ref. [10].

<sup>c</sup>Ref. [19].

<sup>d</sup>This paper.

<sup>e</sup>Ref. [20].

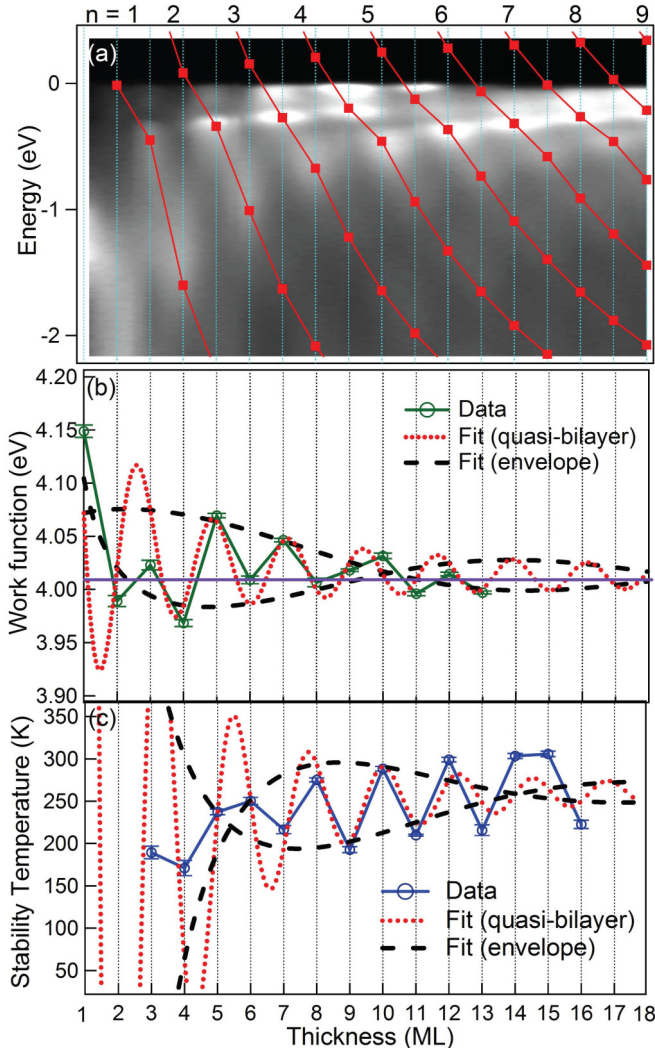


FIG. 3. (Color online) (a) Measured QWS peak intensities as a function of energy and thickness for Pb films on Ge(111). Red squares superimposed are the QWS energy positions derived from Bore-Sommerfeld quantization rule based on the phase shift function extracted from the measurement. (b) Measured work functions as a function of thickness ranging from 1 to 13 ML and the fitted curves. (c) Measured thermal stability temperature (threshold temperature) as a function of thickness ranging from 3 to 16 ML and the fitted curves. The error bars of the measured data are determined from fitting uncertainties.

this phase difference amounts to  $\sim 0.57$  ML, too small to be resolved in the data. The oscillation period of the envelope function is much larger, about 17.4 ML. One-fourth of this period, 4.4 ML, is easily observed and matches our data well.

### 1. 1/4 period phase offset and node positions

Figure 3(a) presents the QWS energy positions as a function of thickness [23]. The thickness-dependent QWS energies are governed by the Bohr-Sommerfeld quantization rule as

$$2k_{\perp}(E)Nd + \Phi = 2n\pi, \quad (4)$$

where  $\Phi$  is the summation of  $\Phi_s$  and  $\Phi_i$ , which represent the phases shifts of the QWS wave functions at the surface and interface, respectively. The former is adopted from a calculation in our analysis [10]; the latter is then extracted through the measured energy positions [the intensity maxima in Fig. 3(a)] via the calculated bulk band dispersion  $E(k_{\perp})$  from  $L$  to  $\Gamma$  with the  $k_{\perp}$  values determined with respect to the  $L$  point. The resulting  $\Phi_i$  is well described by [27]

$$\Phi_i(E) = A' + B'\sqrt{E - E_0}\Theta(E - E_0), \quad (5)$$

with  $A' = -1.14$ ,  $B' = 3.55$ , and  $E_0 = -0.40$  eV. The last quantity  $E_0$  corresponds to the bulk Ge split-off band edge [23]. The red squares in Fig. 3(a) are the QWS energies determined from Eqs. (4) and (5).

In the quantum-well model for freestanding Pb films [19], the work function values were determined considering only the thickness-dependent chemical potentials that exhibit upward sharp cusps at a noninteger thickness, integral multiples of 0.7 ML, where QWS cross the Fermi level. As also observed from the fitting damped oscillation curves in Figs. 3(b) and 3(c), the actual maxima and minima of work functions and surface energies fall mostly between the integer layers. The quantum-well model considers only QWS energy  $E_n$  at the surface zone center ( $k_{\parallel} = 0$ ) on assuming the dispersion of each QWS subband to be purely free-electronlike. A simple expression for the chemical potential  $\mu$  (or Fermi energy) was accordingly derived [19] as

$$\mu = \frac{\rho}{D(\mu)} + \langle E_n \rangle, \quad (6)$$

which reveals the intimate relation between  $\mu$  and  $D(\mu)$ , the DOS at Fermi level, with the electron density  $\rho$  considered as a constant. Therefore, as manifested by Fig. 2 in Ref. [19], the simple picture delivered with the quantum-well model is that the Fermi level crossing of QWS gives rise to a sharp increase of DOS at Fermi level and a sharp drop of work function, namely, a minimum of the work function. The thickness-dependent QWS energy positions shown in Fig. 3(a) are only for discrete  $k_{\perp}$  points projected on the surface zone center  $k_{\parallel} = 0$ . In reality, however, a thin-film property should involve all the electrons occupying the discrete slices of two-dimensional (2D)  $k$  space [15]; an alternative way to approach the thin film property is hence to look into the detailed subband dispersions of QWS. In turn, DOS at the Fermi level is expected to be related to the Fermi level crossing of subbands between surface zone center and the surface zone boundary, namely,

$$D(\mu) = \sum_{n=a}^b D_n^{2D}(E_F), \quad (7)$$

where the sum is over the QWS subbands from the quantum number  $n = a$  to  $n = b$  that pass the Fermi level and  $D_n^{2D}(E_F)$  denotes the 2D DOS per unit area at the Fermi level for each QWS subband. To investigate the work function of Pb films via detailed QWS subbands, we therefore focused on those that cross the Fermi level. It is notable that, unlike the QW model, in which each subband is assumed to be free-electronlike, Pb QWS subbands actually turn downward before reaching surface zone boundary, so part of the Pb occupied QWS

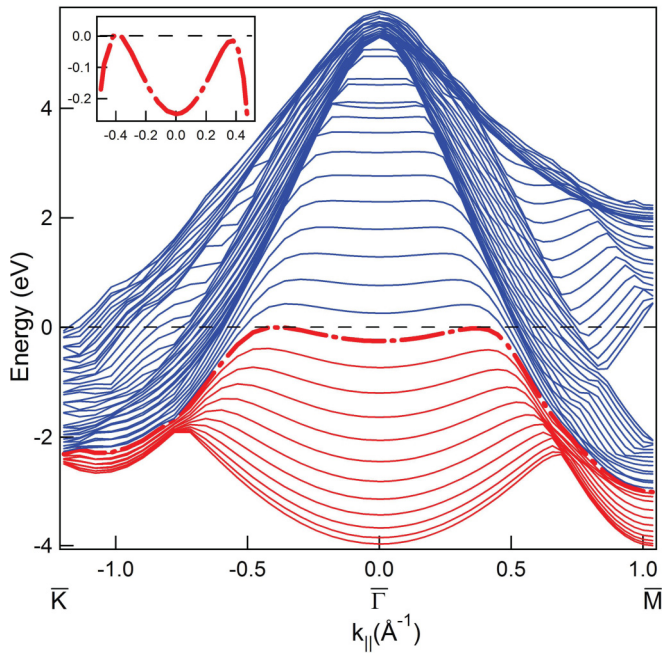


FIG. 4. (Color online) Subband dispersions of bulk Pb projected to the (111) surface in symmetry directions,  $\bar{\Gamma}\bar{K}$  and  $\bar{\Gamma}\bar{M}$ . The inset shows the magnified view of the threshold occupied subband, marked with a long-short dashed line, that passes the Fermi level. The energy region between the bottom of this threshold occupied subband  $-0.250\text{ eV}$  and  $E_F$  at  $k_{\parallel} = 0$  is the effective region for the subbands of HOQWS to contribute to the DOS at Fermi level.

subbands do not pass the Fermi level. On the other hand, the surface energy is pertinent to the filling of the electrons into the occupied subbands at and below Fermi level via this relation

$$E_S = \frac{\left\{ \sum_{n=1}^{n_0} \left[ \int_{E_n}^{E_F \text{ or } E_n^{\max}} \varepsilon_n D_n^{2D}(\varepsilon_n) d\varepsilon_n \right] - V E_{\text{bulk}} \right\}}{2A}, \quad (8)$$

where  $\varepsilon_n$  is the subband energy of the  $n$ th QWS and  $E_{\text{bulk}}$  is the bulk energy density. The film has surface area  $A$  and volume  $V$ . The integral for each occupied QWS subband energy from the lowest ( $n = 1$ ) to the topmost ( $n = n_0$ ) is bounded between the lower limit of subband bottom  $E_n$  and the upper limit of Fermi energy  $E_F$  or the maximum energy of the occupied subband  $E_n^{\max}$ , depending on whether the subband passes the Fermi level or not.

Figure 4 shows the subbands of bulk Pb projected to (111) surface in the two symmetry directions  $\bar{\Gamma}\bar{K}$  and  $\bar{\Gamma}\bar{M}$ . Here, 26 k-points evenly distributed between bulk Pb symmetry points  $L$  and  $\Gamma$  were sampled. As seen, the main contributions to the DOS at the Fermi level are from the subbands, marked in blue, mostly above the Fermi level, which descend passing the Fermi level about  $k_{\parallel} > 0.5\text{ \AA}^{-1}$  and  $k_{\parallel} < -0.5\text{ \AA}^{-1}$ . There are, however, also some partial contributions from the occupied subbands of which the energy positions at the surface zone center range from the Fermi level to  $-0.250\text{ eV}$ , below which the occupied subbands are complete off Fermi level, as seen from the magnified view in the inset. Looking into Figs. 3(a) and 3(b), it is intriguing that the node position of

work function 9 ML, corresponding to the energy position  $-0.197\text{ eV}$  of the QWS, is very close to  $-0.250\text{ eV}$ . This is understandable if we determine the minima of work functions via lowest unoccupied quantum well state (LUQWS) closer to the Fermi level at the surface zone center as their subbands (blue) contribute to the main source of the DOS at the Fermi level. Such is the case for 2, 4, 6, and 8 ML, whereas at 3, 5, and 7 ML, the highest occupied quantum well state (HOQWS) approaches  $-0.250\text{ eV}$  from below; therefore, 9 ML is the threshold thickness for the HOQWS to enter this effective region (between  $E_F$  and  $-0.250\text{ eV}$ ) and to initiate an additional contribution to the DOS at Fermi level through subband dispersions. As one can see, at 11 ML, although the corresponding LUQWS is farther from the Fermi level (out of the energy range in Fig. 3(a)) than the adjacent layers, the corresponding HOQWS at  $-0.126\text{ eV}$  contributes to DOS at Fermi level alternatively to make the work function changeover to a minimum. As for the surface energy, the contributions mainly arise from the upward occupied subbands, marked in red, and partially from the downward subbands, marked in blue, at and below the Fermi level in the range about  $k_{\parallel} > 0.5\text{ \AA}^{-1}$  and  $k_{\parallel} < -0.5\text{ \AA}^{-1}$ , as shown in Fig. 4. The key for the surface energy is the total energy of occupied QWS subbands constituting 2D slices in  $k$  space, which are dominated by the red subbands, rather than the Fermi level passing. When the HOQWS at the surface zone center at an integer thickness is nearer the Fermi level than those of adjacent layers, it should correspond to a local maximum of the surface energy. When the HOQWS just passes the Fermi level at an integer thickness, it should thus be close to a minimum-maximum switching. From Figs. 3(a) and 3(c), at 4 ML, one layer below the node position, the QWS just passes the Fermi level with about  $0.083\text{ eV}$  above it; the surface energy (stability temperature) is a maximum (minimum). At 6 ML, one layer above the node position, where LUQWS is  $0.154\text{ eV}$  above the Fermi level, the surface energy (stability temperature) turns to be a minimum (maximum).

To acquire further insight into the phase-shift relations among work functions  $\phi_w$ , thermal stability  $\phi_{TS}$ , and QWS energies  $\Phi$ , we carried out the calculations of freestanding Pb films with GGA. As Figs. 5(b) and 5(c) show, the node positions determined from crossover points for work functions and surface energies are (3, 12, and 21 ML) and (8, 17, and 26 ML), respectively, distinct from those for Pb films on Ge(111) because of the different thickness-dependent QWS energy positions arising from varied  $\Phi$  values; however, the relative deviation of node positions,  $4\sim 5$  ML, between work function and the surface energy still holds, namely, the  $1/4$  period for the beating envelope. On examining the node position for work function (12 ML) and one layer below the node positions for surface energy (7 ML), a striking result is revealed: not only the same subband arguments used for the Pb films on Ge(111) can also apply, but even the energy positions of HOQWS at 12 ML ( $-0.199\text{ eV}$ ) and LUQWS at 7 ML ( $0.115\text{ eV}$ ) are almost the same as their corresponding ones, 9 ML ( $-0.197\text{ eV}$ ) and 4 ML ( $0.083\text{ eV}$ ), in Fig. 3. The strong interaction between the film and the substrate was speculated possibly to affect the phase relation between the work function and the surface energy [20], but the result above indicates that the distortion of the subbands due to the

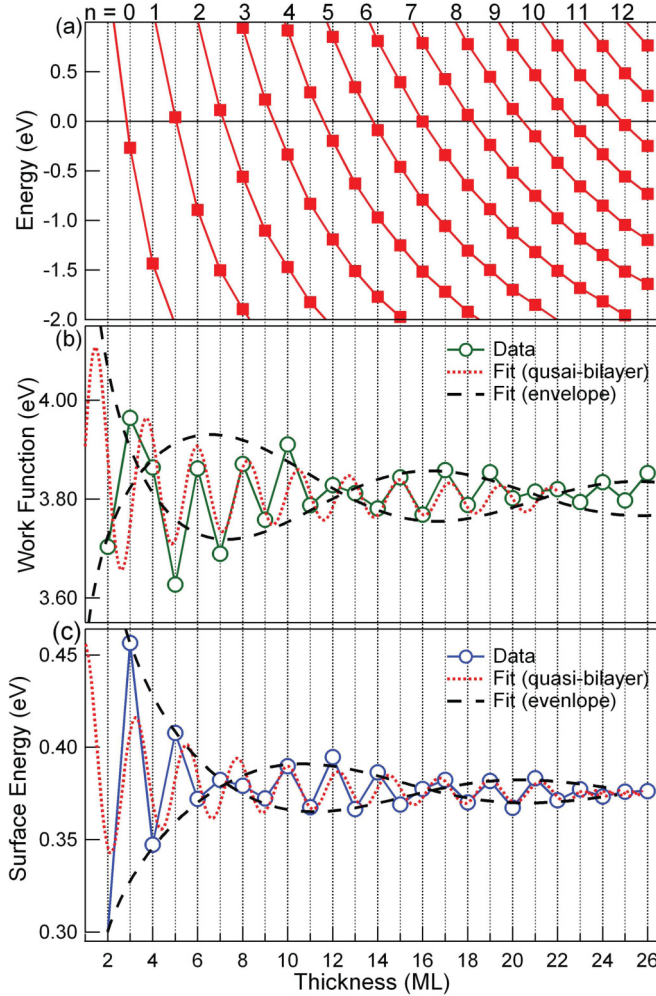


FIG. 5. (Color online) (a) Calculated QWS energies as a function of thickness for freestanding Pb films. (b) Calculated work functions as a function of thickness ranging from 2 to 24 ML and the fitted curves. (c) Calculated surface energies as a function of thickness ranging from 1 to 26 ML and the fitted curves.

interaction between Pb QWS and Ge band edges does not affect the robust relationship among the QWS energy at the surface zone center, the work function, and the surface energy because of the limited distortion of subband dispersions only around the surface zone center [23]. We verify the theoretical quantum-well model [19] again with the results of Pb films on Ge(111) and freestanding Pb films. Quantum-well model assumes the QWS energy at the surface zone center, work function, and surface energy to be continuous functions of a continuous variable, thickness; the work function exhibits a downward cusp centered at the Fermi level crossing of noninteger period that depends on the  $k_F$  values chosen. The determination of the minimum or maximum of the work function for an integer thickness therefore lies in its distance from the adjacent Fermi level crossing. For our case, as mentioned above, the period for the Fermi level crossing is 2.26 ML. From Fig. 3(a), the Fermi level crossing for QWS of  $n = 3$  is at 6.38 ML; the work function at 6 ML should hence be a minimum because of its proximity to the downward cusp. The Fermi level crossing for QWS of  $n = 4$  is at 8.53 ML,

halfway between 8 and 9 ML. It is then reasonable to consider 9 ML as a crossover point for the minimum and maximum. The Fermi level crossing for QWS of  $n = 5$  is 10.72 ML, corresponding to which the work function at 11 ML is expected to be a minimum. These are all confirmed from Fig. 3(b). Regarding the Fermi level crossing of QWS of  $n = 3, 4$ , and 5 in Fig. 5(a) and the corresponding work functions at 9, 12, and 14 ML in Fig. 5(b), one can draw the same argument. Despite an assumption in the quantum-well model that the QWS subbands are only free-electronlike, our approach via detailed subband dispersions clearly points out a correlation of 1/4 period phase offset between thickness dependence of the work function and surface energy with the varied roles of DOS at the Fermi level to both thin-film properties. Our intuitive picture follows. Upon a thickness change, the altered QWS contributions to DOS at the Fermi level induce the instability of charge neutrality so as to cause a shift of Fermi level, namely, the change of work function. The upward shift of the Fermi level (the decrease of the work function) accompanying the sharp increase of DOS at Fermi level serves to relieve the excessive charge. However, the surface energy takes into account all the DOS at and below the Fermi level, so occupied QWS subbands that do not pass the Fermi level still contribute substantially to the surface energy. The work function is hence tied to the hollow Fermi contours, but the surface energy is linked to all the filled 2D  $k$  slices at and below Fermi level. This condition, in turn, causes the crossover positions of the maximum-minimum order (node positions) to differ for both. As for the quantum-well model, the higher sensitivity of the work function to DOS at Fermi level is manifested from Fig. 2 in Ref. [19], where the derivative of work function to DOS at Fermi level  $dW/dD(\mu)$  is overall greater than that of the surface energy  $dEs/dD(\mu)$  simply because the thickness dependence of the work function exhibits a cusp shape with a nearly constant derivative from one noninteger thickness to the adjacent one as opposed to the surface energy of which the derivative varies smoothly between zero and a maximum value. Most importantly, at a noninteger thickness, where the QWS exactly occupied Fermi level, the common sharp variations of the derivative at the tips of both saw teeth [ $D(\mu)$ ] and cusps ( $W$ ) warrant a strong sensitivity between each other.

## 2. Surface dipole effect and work-function amplitudes

By definition, the work function is the energy difference between the energy at the Fermi level and at the vacuum level (VL). The agreement between the quantum-well model and our measured results seems to infer a negligible contribution from the VL to the thickness-dependent work functions. The VL increases with the moment of surface dipoles composed of electron clouds spilled out of the metal surfaces [28]. One typical example is the pushback effect, which decreases the surface dipole length as well as the VL substantially through adsorptions of adsorbates [29]. As phase shifts of QWS at surfaces were considered as charge spillages  $\Delta$  [15], their values are supposed to be proportional to surface dipole effects. The phase shifts calculated by Wei *et al.* show the proportionality with the QWS energies [10]. Similar arguments were derived with the quantum-well model in terms of the relation {Eq. (24) in Ref. [15]} that the charge

TABLE II. Extracted phase shifts of thickness-dependent work function, thermal stability (surface energy), and QWS energies from measurement and calculation.

Pb/Ge(111) (Exp)	Freestanding Pb (Cal) GGA (LDA)
$\phi(E_F)$	1.26
$\phi_w$	0.43
$\phi_{TS}, \phi_{Es}$	-1.18
	-1.98 (-1.29)
	-1.98 (-2.00)
	-0.50 (-0.55)

spillage across the surface is proportional to the Fermi energy. Therefore, the thickness-dependent increment of VL induced by the surface-dipole effect is proportional to the value of thickness-dependent Fermi energy that has a local maximum, at which the QWS crosses the Fermi level. The resultant thickness-dependent work functions would, in turn, have overall smaller amplitudes of minima than those of maxima for the oscillation, as observed according to the data in Fig. 3(b), especially in the thickness range from 4 to 10 ML, with respect to the horizontal line approximately corresponding to the thick-limit value. To estimate the magnitude of the VL change contributed by surface dipole effects, we modified Eq. (24) from Ref. [15] to this form

$$\delta\Delta = \frac{A_{\text{cell}}d}{4\pi N_{\text{val}}} \frac{m}{\hbar^2} (E_F^{\max} - E_F^{\min}) = 0.027d(E_F^{\max} - E_F^{\min}), \quad (9)$$

in which  $A_{\text{cell}}$  is the area of surface unit cell for Pb(111) and  $N_{\text{val}}$  the number of itinerant valence electrons per atom of Pb film ( $N_{\text{val}} = 4$ ). We chose  $\sim 0.1$  eV for  $E_F^{\max} - E_F^{\min}$  between adjacent integer layers. This value is reasonable for the low-thickness regime; the resulting charge spillage change is  $\delta\Delta = 0.0077$  Å via Eq. (9). We then consider the array of the surface dipoles as two parallel plates of opposite charges with the separation equal to the average surface dipole length as well as the charge spillage  $\Delta$ . Then the corresponding VL change  $\delta\text{VL}$  can be approximated by

$$\delta\text{VL} = \frac{q_{\text{dipole}}\delta\Delta}{\varepsilon_0 A_{\text{cell}}} e, \quad (10)$$

where the charge of one surface dipole per atom  $q_{\text{dipole}}$  is taken to be  $0.5e$  on referring to the average charge density spilled off the film boundary [Fig. 3(b) of Ref. [15]]. Consequently,  $\delta\text{VL} = 0.066$  eV, which is less than 0.1 eV so that this value is not large enough to affect the work-function bilayer oscillation as well as its phase shift, determined on considering only the chemical potential. As the difference between the Fermi energies of adjacent integer layers decreases with increasing thickness, the variation of VL change correspondingly attenuates to zero in the thick limit.

### 3. Universal phase relation

The phase shifts extracted from thickness-dependent work functions  $\phi_w$ , thermal stability  $\phi_{TS}$  (differing from  $\phi_{Es}$  by  $\pm\pi$ ), and QWS energies  $\Phi$  for both values measured from Pb films on Ge(111) and calculated from the freestanding Pb films are summarized in Table II, which shows that the 1/4 period difference  $\sim \pm 1.5$  or  $\pm \frac{\pi}{2}$  ( $\phi_w - \phi_{TS}$  or  $\phi_w - \phi_{Es}$ ) between oscillations of work function and thermal stability

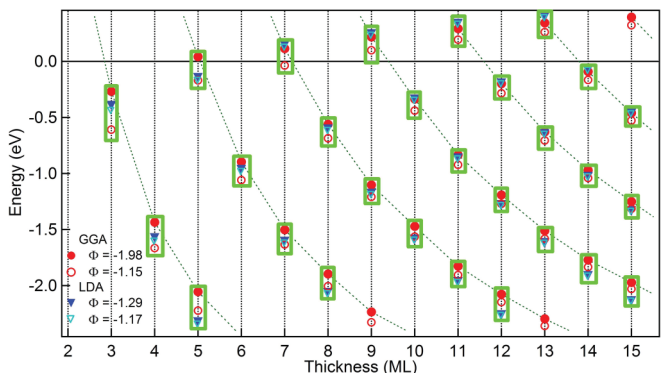


FIG. 6. (Color online) Comparison of calculated (GGA and LDA) QWS energy positions derived from phase shifts with various constant offsets.

(surface energy) is in common independent of the existence of a substrate. However, the relations between the total phase shift of QWS at the Fermi level  $\Phi(E_F)$  and those of the work functions and surface energies [ $\phi_w$  and  $\phi_{TS}$  ( $\phi_{Es}$ )] seem random; the difference between  $\Phi$  and  $\phi_w$  is  $\sim 0.83$  from the measured data and  $\sim 0$  from the calculation with GGA. The phase-shift values extracted from the calculation via the LDA show an improved agreement with measurement with intermediate value  $\sim 0.71$ . One must be aware that the physical origins of  $\Phi$  and  $\phi_w$  (or  $\phi_{Es}$ ) differ; the former refers to the total phase shift of QWS wave functions at the surfaces and interfaces, whereas the latter refers to the phase shifts of damped sinusoidal functions. Nevertheless, the quantization condition, Eq. (4), for the wave vectors as well as energies of QWS provides a special interlock channel for them. As we have demonstrated, the thickness-dependence of work functions and surface energies are both closely related to the energy positions of QWS—their phase shifts should thus be linked to  $\Phi$  through Eq. (4) in a particular form. To check whether  $\Phi$  has a definite relation with  $\phi_w$  and hence  $\phi_{TS}$  ( $\phi_{Es}$ ), we compare the QWS energy positions (filled circles and triangles) derived from the originally calculated phase shift with those (empty circles and triangles) derived from the phase-shift values with the intended offsets of 0.83 and 0.12 to make their deviation from the corresponding  $\phi_w$  values the same as that of measurement. As shown in Fig. 6, the four energy positions of the same quantum number and thickness are grouped within a rectangular frame of which the height is proportional to the largest deviation of the energies. Except the small coverage below 5 ML, the deviation is apparently small with respect to the large difference in  $\Phi$ . That is, unlike the robust values of  $\phi_w$  and  $\phi_{TS}$  ( $\phi_{Es}$ ) with respect to the variation of amplitudes of work functions and surface energies, the values of  $\Phi$  are overall very sensitive to a slight variation of QWS energy positions, which can be caused by a varied resolution of measurements or the varied approximations in calculations. Moreover, in the case of Pb films on Ge(111), the strong electronic interaction between the QWS and the substrate bands produces also an evident shift of QWS energies [23]. A definite relation between  $\Phi$  and  $\phi_w$  is hence extracted less easily than that between  $\phi_w$  and  $\phi_{TS}$  ( $\phi_{Es}$ ), but the definite and universal deviation between  $\Phi(E_F)$  and  $\phi_w$  may fall within the range 0 to 0.83.

#### IV. SUMMARY

We explored the relations among the thickness-dependent QWS energies, surface energies, and the work functions of ultrathin films via a comparison between measured results of Pb films on Ge(111) ranging from 1 to 16 ML and those calculated based on freestanding Pb films, from both of which the phase shifts of QWS energies, surface energies, and the work functions are extracted through fitting; the phase shift difference of a 1/4 period between surface energies and work functions, as predicted with the quantum-well model, is confirmed. Upon close examination of the energy positions of HOQWS and LUQWS relative to the Fermi level around the crossover thickness (node positions) with the aid of detailed subband dispersions, this 1/4 period difference can be attributed to the higher sensitivity of the work function to the variation of the DOS at Fermi level than the surface energy. The different sensitivity indicates the two distinct roles of the DOS at Fermi level to them; the former is for pinning to maintain charge neutrality, and the latter, as well as the DOS of other occupied energy levels, is for filling in terms of energy stability. The detailed-subband approach considers discrete integer thickness and 2D QWS subbands, but the genetic quantum-well model employs continuous thickness and one-dimensional QWS at the surface zone

center. Both apply satisfactorily to the measured result, Pb films on Ge(111), and the calculated result, freestanding Pb films. This agreement indicates that the 1/4 period phase difference is expected to be a universal property for thin-film systems of all kinds. The investigation of other thin-film systems is still necessary to consolidate this picture fully. The surface dipoles due to the charge spillage of QWS are proved to have no relevant effect on the phase shifts of work-functions oscillations. Previous reports of STM measurements on Pb films on Si(111) [19–21] have disagreements on the phase relation between the work functions and the surface energies. We speculate an enhanced surface dipole effect drawn by the STM tip. A careful comparison of thickness-dependent QWS energies over varied QWS phase-shift offsets indicates the possible existence of a universal relation among the phase shifts of QWS, work functions, and surface energies.

#### ACKNOWLEDGMENTS

National Science Council of Taiwan (Grant Nos. NSC 98-2112-M-007-017-MY3 and NSC 102-2112-M-007-009-MY3) provided support. All the experimental work was performed at the National Synchrotron Radiation Research Center of Taiwan. We sincerely appreciate helpful discussions with T.-C. Chiang.

- 
- [1] J. J. Paggel, C. M. Wei, M. Y. Chou, D.-A. Luh, T. Miller, and T.-C. Chiang, *Phys. Rev. B* **66**, 233403 (2002).
  - [2] D.-A. Luh, T. Miller, J. J. Paggel, M. Y. Chou, and T.-C. Chiang, *Science* **292**, 1131 (2001).
  - [3] S.-J. Tang, W.-K. Chang, Y.-M. Chiu, H.-Y. Chen, C.-M. Cheng, K.-D. Tsuei, T. Miller, and T.-C. Chiang, *Phys. Rev. B* **78**, 245407 (2008).
  - [4] S.-J. Tang, C.-Y. Lee, C.-C. Huang, T.-R. Chang, C.-M. Cheng, K.-D. Tsuei, and H.-T. Jeng, *Appl. Phys. Lett.* **96**, 103106 (2010).
  - [5] D.-A. Luh, T. Miller, J. J. Paggel, and T.-C. Chiang, *Phys. Rev. Lett.* **88**, 256802 (2002).
  - [6] Y.-F. Zhang, J.-F. Jia, T.-Z. Han, Z. Tang, Q.-T. Shen, Y. Guo, Z. Q. Qiu, and Q.-K. Xue, *Phys. Rev. Lett.* **95**, 096802 (2005).
  - [7] Y. Guo, Y.-F. Zhang, X.-Y. Bao, T.-Z. Han, Z. Tang, L.-X. Zhang, W.-G. Zhu, E. G. Wang, Q. Niu, Z. Q. Qiu, J.-F. Jia, Z.-X. Zhao, and Q.-K. Xue, *Science* **306**, 1915 (2004).
  - [8] L. Aballe, A. Barinov, A. Locatelli, S. Heun, and M. Kiskinova, *Phys. Rev. Lett.* **93**, 196103 (2004).
  - [9] F. K. Schulte, *Phys. Stat. Sol.* **79**, 149 (1977); *Surf. Sci.* **55**, 427 (1976).
  - [10] C.-M. Wei and M.-Y. Chou, *Phys. Rev. B* **66**, 233408 (2002).
  - [11] Yu Jia, Biao Wu, H. H. Weitering, and Z. Zhang, *Phys. Rev. B* **74**, 035433 (2006).
  - [12] Y. Han and D.-J. Liu, *Phys. Rev. B* **80**, 155404 (2009).
  - [13] H. Hong, *Phys. Rev. Lett.* **90**, 076104 (2003).
  - [14] P. Czoschke, H. Hong, L. Basile, and T.-C. Chiang, *Phys. Rev. Lett.* **93**, 036103 (2004).
  - [15] P. Czoschke, H. Hong, L. Basile, and T.-C. Chiang, *Phys. Rev. B* **72**, 075402 (2005).
  - [16] M. H. Upton, C. M. Wei, M. Y. Chou, T. Miller, and T.-C. Chiang, *Phys. Rev. Lett.* **93**, 026802 (2004).
  - [17] M. M. Özer, Y. Jia, B. Wu, Z. Zhang, and H. H. Weitering, *Phys. Rev. B* **72**, 113409 (2005).
  - [18] D. A. Ricci, T. Miller, and T.-C. Chiang, *Phys. Rev. Lett.* **95**, 266101 (2005).
  - [19] T. Miller, M. Y. Chou, and T.-C. Chiang, *Phys. Rev. Lett.* **102**, 236803 (2009).
  - [20] J. Kim, C. Zhang, J. Kim, H. Gao, M.-Y. Chou, and C.-K. Shih, *Phys. Rev. B* **87**, 245432 (2013).
  - [21] Y. Qi, X. Ma, P. Jiang, S. Ji, and Y. Fu, J.-F. Jia, Q.-K. Xue, and S.B. Zhang, *Appl. Phys. Lett.* **90**, 013109 (2007).
  - [22] J. Kima, S. Qina, W. Yaob, Q. Niua, M.-Y. Chou, and C.-K. Shih, *Proc. Natl. Acad. Sci. USA* **107**, 12761 (2010).
  - [23] S.-J. Tang, C.-Y. Lee, C.-C. Huang, T.-R. Chang, C.-M. Cheng, K.-D. Tsuei, H.-T. Jeng, V. Yeh, and T.-C. Chiang, *Phys. Rev. Lett.* **107**, 066802 (2011).
  - [24] H. Morikawa, I. Matsuda, and S. Hasegawa, *Phys. Rev. B* **77**, 193310 (2008).
  - [25] J. P. Perdew and Y. Wang, *Phys. Rev. B* **45**, 13244 (1992).
  - [26] J. P. Perdew and A. Zunger, *Phys. Rev. B* **23**, 5048 (1981).
  - [27] D. A. Ricci, Y. Liu, T. Miller, and T.-C. Chiang, *Phys. Rev. B* **79**, 195433 (2009).
  - [28] H. Ishii, K. Sugiyama, E. Ito, and K. Seki, *Adv. Mater.* **11**, 605 (1999).
  - [29] M.-K. Lin, Y. Nakayama, C.-Y. Wang, J.-C. Hsu, C.-H. Pan, S. I. Machida, T.-W. Pi, H. Ishii, and S.-J. Tang, *Phys. Rev. B* **86**, 155453 (2012).